

# Axial optical trapping forces on two particles trapped simultaneously by optical tweezers

Shenghua Xu, Yinmei Li, and Liren Lou

Optical tweezers, which utilize radiation pressure to control and manipulate microscopic particles, are used for a large number of applications in biology and colloid science. In most applications a single optical tweezers is used to control one single particle. However, two or more particles can be trapped simultaneously. Although this characteristic has been used in applications, no theoretical analysis of the trapping force or the status of the trapped particles is available to our knowledge. We present our calculation, using a ray optics model, of the axial trapping forces on two rigid particles trapped in optical tweezers. The spherical aberration that results from a mismatch of the refractive indices of oil and water is also considered. The results show that the forces exerted by the optical tweezers on the two particles will cause the two particles to touch each other, and the two particles can be stably trapped at a joint equilibrium point. We also discuss the stability of axial trapping. The calculation will be useful in applications of optical tweezers to trap multiple particles. © 2005 Optical Society of America

OCIS codes: 140.7010, 140.0140, 080.2710.

## 1. Introduction

Optical trapping is a novel technique that utilizes radiation pressure to control and manipulate microscopic particles. A single-beam gradient-force optical trap, also known as tweezers, was first demonstrated by Ashkin *et al.*<sup>1</sup> When a laser beam is focused tightly, large intensity gradients are created in both the axial and the transverse directions. A dielectric particle can then be confined near the beam focus by the gradient force.

Since its invention, optical tweezers has been widely used in many research fields, such as biology<sup>2–4</sup> and colloid science.<sup>5–8</sup> For these applications, accurate characterization of the properties of the trapping force is necessary. The trapping force of optical tweezers was studied previously theoretically with either a ray-optics (RO) model<sup>9–11</sup> or an electromagnetic model<sup>12</sup> for large particles and small particles, respectively. Recently these forces were also calculated from scattering theory for the

intermediate-size regime.<sup>13</sup> Various computing methods have also been developed for calculating the trapping force.<sup>14</sup> The spherical aberration that results from the refractive-index mismatch between the oil and the medium in which the particles are suspended was also considered in the calculations with these models.<sup>13,15,16</sup>

In most applications an optical tweezers is used to control only one single particle. Recently some techniques were developed to achieve multiple trapping sites by use of Bessel beams<sup>17</sup> or computer-designed holograms.<sup>18</sup> Also, it is known that one single-beam gradient-force optical trap can control more than one particle simultaneously. However, this characteristic is usually thought of as a nuisance. However, this property has been used to investigate the stability ratio of polystyrene dispersion, in which two particles were trapped simultaneously by an optical tweezers.<sup>19</sup> Knowledge of the trapping forces that act on the two particles is of importance for predicting and understanding the movement and the interaction of the two trapped particles and is also useful for both research on the character of multiple trapping and on its applications. However, the characteristics of optical tweezers when they are trapping two particles have never been discussed to our knowledge.

In this paper we will use the RO model to calculate the axial trapping forces on two rigid particles trapped by optical tweezers. Spherical aberration is also considered in the calculation.

Y. Li (liyimin@ustc.edu.cn), S. Xu, and L. Lou (loulr@ustc.edu.cn) are with the Department of Physics, University of Science and Technology of China, Hefei, 230026, Anhui, China. S. Xu and Y. Li are also with the Hefei National Laboratory for Physical Sciences at Microscale, University of Science and Technology of China, Hefei, 230026, Anhui, China.

Received 13 August 2004; revised manuscript received 8 November 2004; accepted 8 November 2004.

0003-6935/05/132667-06\$15.00/0

© 2005 Optical Society of America

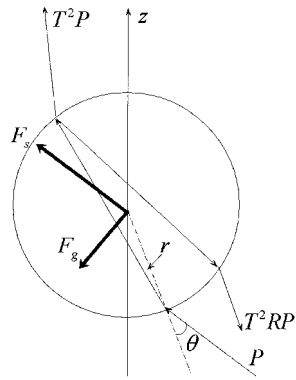


Fig. 1. RO model for optical trapping (after Ashkin<sup>9</sup>). Scattering force  $F_s$  points in the direction of the incident ray; gradient force  $F_g$  is perpendicular to the direction of the incident ray.  $\theta$  is the angle of incidence;  $r$  is the angle of refraction. The intensities of the reflected and refracted rays are determined by Fresnel reflection  $R$  and transmission  $T$  coefficients, respectively, and by power  $p$  of the incident ray. The parameters of the reflected and transmitted rays out of the bead can also be determined from this figure.

## 2. Calculation of the Trapping Force

Using the RO model, one may calculate the total force exerted on a particle by calculating the forces of single rays that strike the particle and then integrating the forces of all the rays of the beam acting on the particle. According to Fresnel laws, a ray incident upon a particle will be partly transmitted and partly reflected at the surface. Each refraction and reflection will transfer momentum and exert force on the particle. The principal relationship between the trapping force and the laser power is  $F = QnP/c$ , where  $n$  is the refractive index of the surrounding medium,  $P$  is the laser power, and  $c$  is the speed of light in free space.  $Q$  is a normalized trapping force, which is generally termed trapping efficiency.

It was shown by Ashkin that the force produced by a single ray that impinges upon a bead can be divided into two parts, a ray-scattering force parallel to the incident ray and a ray-gradient force perpendicular to the incident ray.<sup>9</sup> The trapping efficiency of the two parts can be written as

$$Q_s = 1 + R \cos(2\theta) - \frac{T^2[\cos(2\theta - 2r) + R \cos(2\theta)]}{1 + R^2 + 2R \cos(2r)}, \quad (1)$$

$$Q_g = R \sin(2\theta) - \frac{T^2[\cos(2\theta - 2r) + R \sin(2\theta)]}{1 + R^2 + 2R \cos(2r)}, \quad (2)$$

where  $\theta$  is the angle of incidence,  $r$  is the angle of refraction, and  $R$  and  $T$  are the Fresnel reflection and transmission coefficients, respectively. Figure 1 shows the geometry of the propagation of light in a system with a bead in a uniform medium.

In the usual optical tweezers the light passes through immersion oil and glass before it enters water, as shown in Fig. 2. The oil and the glass have

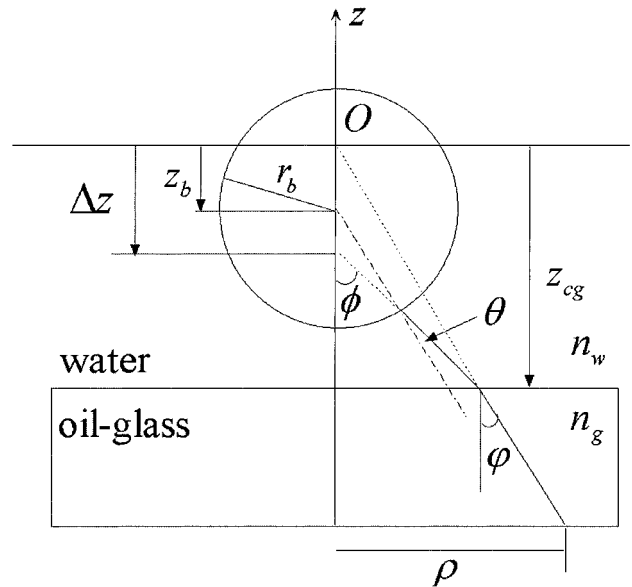


Fig. 2. Schematic illustration of light in an optical tweezers system including a glass–water interface (after Fallman and Axner<sup>16</sup>). The parameters marked in the figure are needed in the calculation and are discussed in the text.

identical refractive indices  $n_g$ , whereas the index of refraction of water is  $n_w$ , which is lower than  $n_g$ . This index mismatch causes spherical aberration, which is considered automatically through ray tracing. In the figure the  $z$  axis lies along the direction of propagation of the beam, which is upward and perpendicular to the glass–water interface. In the figure a typical ray emerging from an oil-immersion objective and impinging upon a bead of radius  $r_b$  is traced. The ray is coplanar with the beam axis, exits the pupil of the objective at a radial coordinate  $\rho$ , and is incident onto the interface between oil–glass and water at incident angle  $\phi$  and refractive angle  $\phi$ . All the incident rays on the glass–water interface can be prolonged to intersect the beam axis at the ideal focal point  $O$ , which is the origin of the coordinate system in Fig. 2. The distance between the glass–water interface and  $O$  is  $z_{cg}$ . The refracted ray will intersect the axis at a point that is a distance  $\Delta z$  from point  $O$  in the absence of the bead. The distance between the center of the bead and point  $O$  is denoted  $z_b$ . The parameters are shown in Fig. 2.

Then incident angle  $\theta$  of a specific ray on the surface of the bead can be expressed in terms of angle  $\phi$  and various geometric parameters as follows:

$$\sin(\theta) = \frac{z_b - \Delta z}{r_b} \sin(\phi). \quad (3)$$

By geometric reasoning,  $\Delta z$  can be written as

$$\Delta z = z_{cg} \left\{ 1 - \frac{n_w}{n_g} \left[ \frac{1 - \eta^2(\text{NA}/n_w)^2}{1 - \eta^2(\text{NA}/n_g)^2} \right]^{1/2} \right\}, \quad (4)$$

where NA is the numerical aperture of the objective and  $\eta$  is the relative pupil coordinate defined in terms of the radius of the exit pupil of the objective,  $\rho_p$ , as

$$\eta = \rho / \rho_p. \quad (5)$$

The relationship of  $\phi$  to  $\eta$  is

$$\sin(\phi) = \frac{\text{NA}}{n_w} \eta. \quad (6)$$

The laser beam is assumed to have a truncated Gaussian intensity distribution at the position of the exit pupil:

$$I(\rho) = \begin{cases} I_0 \exp(-2\rho^2/w_0^2) & \rho \leq \rho_p \\ 0 & \rho > \rho_p \end{cases}, \quad (7)$$

where  $I_0$  is the intensity at the center of the beam and  $w_0$  is the width of the beam at the exit pupil of the objective. In the calculation that follows, we take  $w_0$  equal to  $\rho_p$ , which is appropriate for most optical tweezers.

Then  $Q_s$  and  $Q_g$  can be calculated from Eqs. (1) and (2) by use of system parameters  $n_g$ ,  $n_w$ , NA,  $z_{cg}$ ,  $r_b$ , and  $\eta$ .

If two particles are trapped simultaneously by an optical tweezers, they will align along the axis because the transverse trapping force is much larger than the axial trapping force. Then the propagation of the rays will have different probabilities, as follows: Some rays will strike the first particle, and the transmitted and reflected rays will interact with the second particle if they impinge upon it. Some rays will not strike the first particle but will impinge upon the second particle. Also, some rays may not impinge upon either particle and thus will have no effect on the trapping force. For calculation of the trapping force on the second particle, one must first calculate the geometric parameters of the transmitted and reflected rays of the first particle according to Figs. 1 and 2.

Suppose that the ray incident upon the first bead forms an angle  $\phi_1$  with respect to the axis; the corresponding angles of incidence and refraction on the first particle will be  $\theta_1$  and  $r_1$ , respectively, and it can be shown by geometric reasoning that the angle of the reflection ray with respect to the axis will be  $\pi + \phi_1 + 2\theta_1$ . The reflection ray will intersect the beam's axis in the absence of a bead. The distance between the intersection with the center of the first bead can be calculated to be  $r_b \sin(\theta_1)/\sin(\pi + \phi_1 + 2\theta_1)$ . The intensity of the reflection ray is  $R_p$ , where  $p$  is the intensity of the incident ray.

The rays reflected in the particle  $m$  times and finally transmitted through the bead have intensity  $T^2 R^m p$ . The angles of the rays with respect to the axis are  $2\theta_1 + \phi_1 - 2r_1 - m(\pi + 2r_1)$ . The transmitted rays will intersect the beam axis in the absence of a bead. The distances between the intersections and the cen-

ter of the first bead can be calculated to be  $r_b \sin(\theta_1)/\sin[2\theta_1 + \phi_1 - 2r_1 - m(\pi + 2r_1)]$ .

Using these parameters, one can also deduce the angle of incidence on the second particle by an analysis similar to that described above.

In the calculation, the total trapping force exerted on the first particle is the vector summation over the forces that are due to the rays that impinge upon the bead. The total force exerted on the second particle is the vector summation over the forces that are due to the rays that do not impinge upon the first bead and the reflected and transmitted rays that exit the first bead.

In the calculation for the trapping force on the second particle, the contribution of the transmitted rays can be ignored if the intensity is small compared with that of the initial ray that impinges upon the first particle. For the calculations in this paper, the transmitted rays are ignored when  $T^2 R^m < 0.01$ . As only on-axis trapping is considered in this study, each ray will contribute amounts  $Q_s \cos(\phi)$  and  $-Q_g \sin(\phi)$  to the total scattering and gradient forces, respectively.

### 3. Results and Discussion

When a laser beam exerts forces on two rigid particles and traps them in the axial direction, there are two possible results for the two particles. There may be two separate equilibrium points or the two particles may be trapped at a joint equilibrium point, in which case the two particles will touch each other as a result of the trapping force. Using the calculation method mentioned above, we can test which of the two different possibilities can happen.

In the calculation, parameters that are typical of an ordinary optical tweezers system are used. The spherical particles have a refractive index of 1.55. The refractive index of water is 1.33. The index of refraction of glass and of immersion oil is taken as 1.516. The width of the beam at the exit pupil,  $w_0$ , is taken to be equal to the radius of the exit pupil,  $\rho_p$ . In the calculation the NA is a constant, taken to be 1.25. As was mentioned in Section 2, point O (as shown in Fig. 2) is the origin of the coordinate system for calculating the positions of particles.

Figure 3 shows the force exerted on the second particle if the first particle is assumed to be trapped at its own equilibrium point and the second particle is a distance (larger than  $2r_b$  for center-to-center distance) apart from the first particle. In Figs. 3(a) and 3(b) the parameters  $z_{cg}$  are taken to be  $-3r_b$  and  $-4r_b$ , respectively. The equilibrium points of the first particle ( $z_b$  in Fig. 2) are calculated to be  $-0.480r_b$  and  $-0.694r_b$ , respectively, with the parameters in Figs. 3(a) and 3(b). The leftmost limits of the curves correspond to second particles in contact with the first particles, such that the positions of the second particle are  $1.520r_b$  ( $-0.480r_b + 2r_b$ ) and  $1.306r_b$  ( $-0.694r_b + 2r_b$ ) for the leftmost limits of the curves in Figs. 3(a) and 3(b), respectively. It is shown by the curves that, when the second particle is near the first

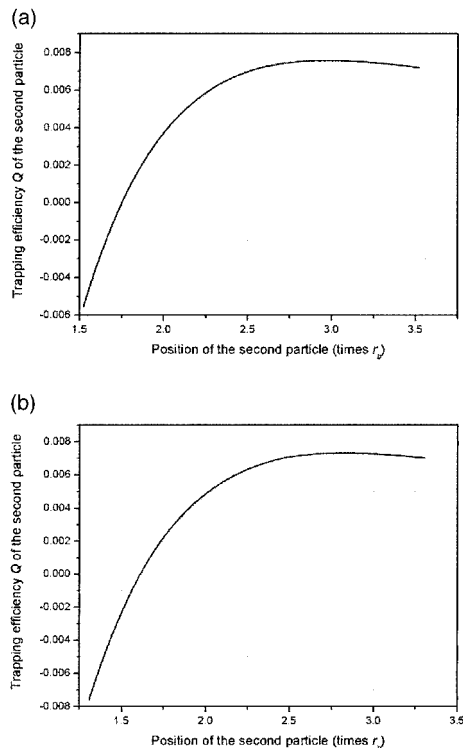


Fig. 3. Trapping force exerted on the second particle if the first particle is assumed to be trapped at its own equilibrium point and is not in contact with the second particle. The leftmost limits of the curves are the equilibrium points of the first particle plus the diameter of the particle. (a)  $z_{cg} = -3r_b$ ; (b)  $z_{cg} = -4r_b$ .

particle, the force exerted on the second particle is negative, which means that the force will draw the second particle into contact with the first particle. The second particle will have no equilibrium point, which means that the assumption that the two particles would be trapped at different equilibrium points is not appropriate. Figure 3 also shows that, when the position of the second particle is below  $1.750r_b$  or  $1.611r_b$  (correspondingly the distance between the two particles will be  $2.230r_b$  or  $2.305r_b$ ), the second particle will be sucked into the optical tweezers and will finally be in contact with the first particle.

When the second particle is sucked in, the two particles will be trapped at the joint equilibrium point, where the forces exerted on the two particles will be of the same magnitude but opposite directions. The calculation shows that, when the two particles are trapped at the joint equilibrium point, the positions of the first particle are  $z_{b1} = -0.570r_b$  and  $z_{b1} = -0.865r_b$  and the positions for the second particle are  $z_{b1} = 1.430r_b$  and  $z_{b1} = 1.135r_b$ , respectively, for  $z_{cg}$  to be  $-3r_b$  and  $-4r_b$ . And the trapping efficiencies that bind the two particles together are 0.0082 and 0.0132.

When the two particles are trapped at the joint equilibrium point the first particle is stable because it is difficult for the particle to escape downward from the trap.<sup>16</sup> Then it is important to calculate the force

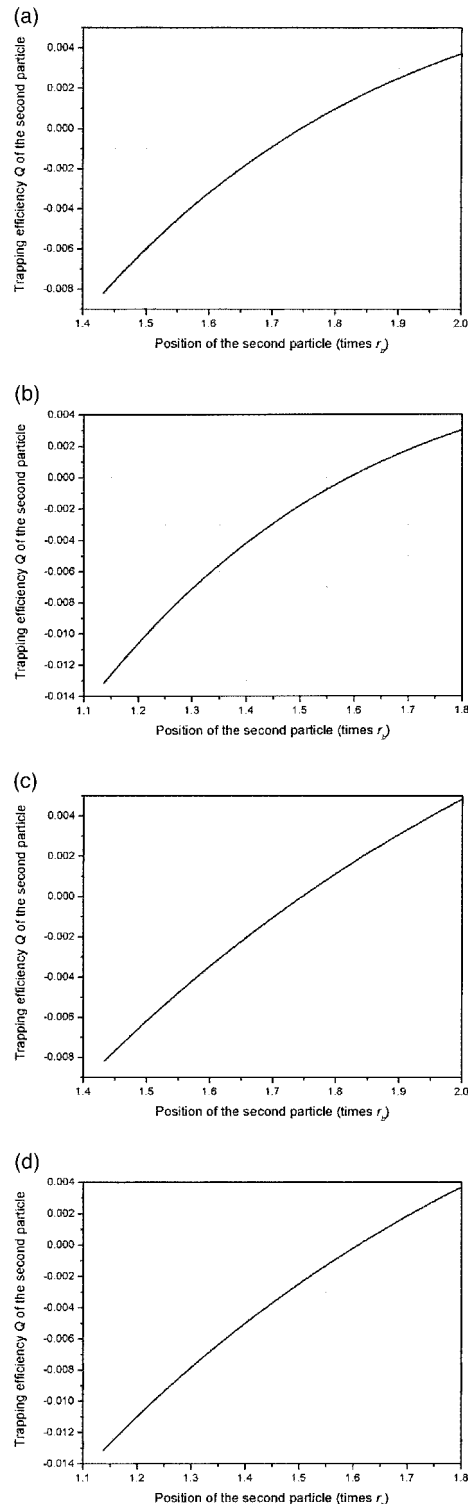


Fig. 4. Trapping force exerted on the second particle. The leftmost limits of the curves are the equilibrium points of the first particle plus the diameter of the particle. (a), (c)  $z_{cg} = -3r_b$ ; (b), (d)  $z_{cg} = -4r_b$ . (a), (b) The first particle stays at the position corresponding to joint equilibrium. (c), (d) The first particle is always in contact with the second particle.

on the second particle to study the stability of the trapping. It can be shown that, when the second par-



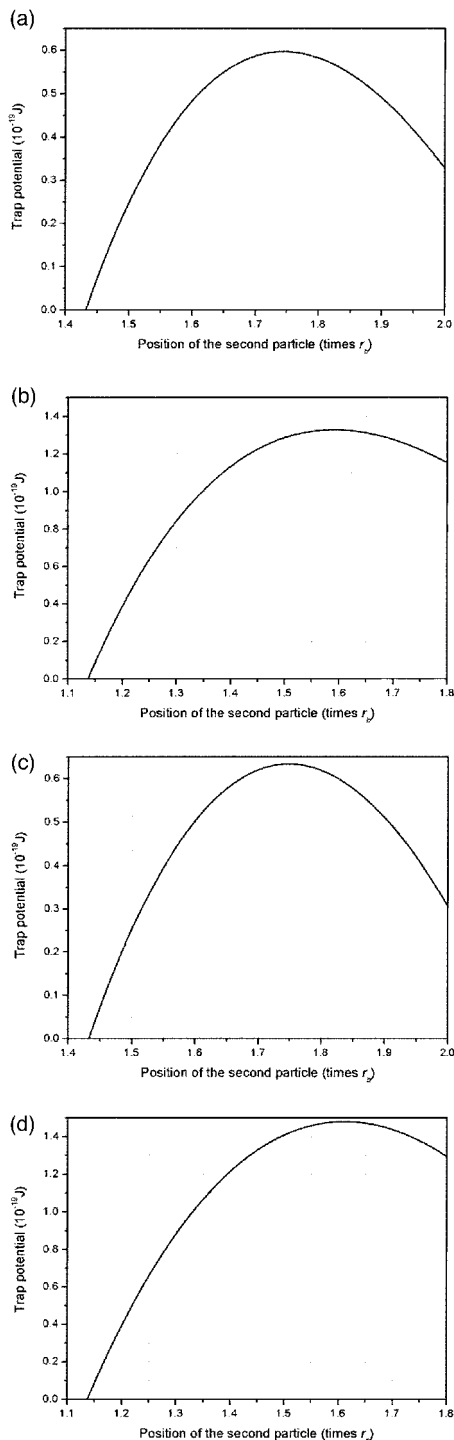


Fig. 5. Curves of the trapping potential of the second particle; the power of the laser beam is assumed to be 10 mW. The potentials on the positions where the two particles are at equilibrium points are taken to be 0. (a), (c)  $z_{cg} = -3r_b$ ; (b), (d)  $z_{cg} = -4r_b$ . (a), (b) The first particle stays at the position corresponding to joint equilibrium. (c), (d) The first particle is always in contact with the second particle.

ticle moves upward from the joint equilibrium point, the first particle will have a tendency to move upward because of the trapping force. However, it is not easy to determine the position of the first particle because of the presence of Brownian motion. The two limited

possibilities for the position of the first particle are that (1) the first particle stays at the position in which it is when the two particles are trapped at the joint equilibrium point and (2) the first particle is always in contact with the second particle. By analyzing and comparing the trapping force on the second particle in terms of these two limited possibilities, we can gain insight into the stability of the trapping. For the situation when the two particles are in contact, one can calculate the force on the two-particle complex by simply adding the forces on the two particles.

Figure 4 shows the curves of the forces exerted on the second particle. Figures 4(a) and 4(b) describe the situation in which the first particle stays at the position corresponding to joint equilibrium and Figs. 4(c) and 4(d) represent the situation in which the first particle is always in contact with the second particle. For the cases in Figs. 4(a) and 4(c),  $z_{cg}$  is taken to be  $-3r_b$ ; whereas for Figs. 4(b) and 4(d),  $z_{cg}$  is  $-4r_b$ . The corresponding potentials of the second particle are shown in Fig. 5, for which the power of the laser beam is taken to be 10 mW.

The leftmost limits of the curves are the positions of the center of the second particle when the two particles are trapped at the joint equilibrium point. For Fig. 5 the potentials of the leftmost limits of the curves are taken to be 0, as these limits are the positions where the two particles are at an equilibrium point. It can be seen from the figures that the difference between the two limited possibilities for the position of the first particle is small. The height of the potential barrier in Fig. 5 is at least  $0.6 \times 10^{-19}$ , which is  $\sim 15$  kT (where  $T = 300$  K), showing that the second particle can be stably trapped by the optical tweezers with a laser beam of 10-mW power. Figures 4 and 5 also show that the height of the potential barrier and the trapping area for  $z_{cg} = -4r_b$  are larger than those of  $-3r_b$ . This means that the farther the distance of the ideal focal point of the laser beam from the glass-water interface, the more stable the trapping of the second particle.

#### 4. Conclusions

To understand the behavior of two particles in optical tweezers, we have examined the axial forces that act on the two particles, using a ray-optics model for the first time to our knowledge. Using this model, we can deduce the track of a single ray in the two particles by geometric reasoning, which makes it easy to sum the forces of all rays to get the total force.

From the calculation it can be concluded that the forces exerted by the optical tweezers on the two particles will make the two particles come into contact with each other. Then the two particles can be stably trapped at a joint equilibrium point, where the forces exerted on the two particles are of the same magnitude but opposite directions. The calculation results also show that one can improve the stability of the axial trapping by increasing the distance between the glass-water interface and the ideal focal point O of the laser beam. However, the RO model is not accu-

rate enough for a particle that is not much larger than a wavelength, such as the 1- $\mu\text{m}$ -diameter particles used in the research reported in Ref. 19. Further study is needed to calculate the behavior of two particles in optical tweezers under those circumstances. More-detailed studies that consider other interactions of the two particles will also make for a clearer understanding of the behavior of two particles in optical tweezers.

This research is supported by grant 20273065 from the National Natural Science Foundation of China and by the "Knowledge Innovation Program" of the Chinese Academy of Sciences.

## References

1. A. Ashkin, J. M. Dziedzic, J. E. Bjorkholm, and S. Chu, "Observation of a single-beam gradient force optical trap for dielectric particles," *Opt. Lett.* **11**, 288–290 (1986).
2. A. Ashkin and J. M. Dziedzic, "Optical trapping and manipulation of viruses and bacteria," *Science* **235**, 1517–1520 (1987).
3. A. Ishijima, H. Kojima, T. Funatsu, M. Tokunaga, H. Higuchi, H. Tanaka, and T. Yanagida, "Simultaneous observation of individual ATPase and mechanical events by a single myosin molecule during interaction with actin," *Cell* **92**, 161–171 (1998).
4. M. D. Wang, "Manipulation of single molecules in biology," *Curr. Opin. Biotechnol.* **10**, 81–86 (1999).
5. J. C. Crocker, "Measurement of the hydrodynamic corrections to the Brownian motion of two colloidal spheres," *J. Chem. Phys.* **106**, 2837–2840 (1997).
6. J. C. Crocker and D. G. Grier, "Microscopic measurement of the pair interaction potential of charge-stabilized colloid," *Phys. Rev. Lett.* **73**, 352–355 (1994).
7. D. G. Grier, "Optical tweezers in colloid and interface science," *Curr. Opin. Colloid Interface Sci.* **2**, 264–270 (1997).
8. R. J. Owen, J. C. Crocker, R. Verma, and A. G. Yodh, "Measurement of long-range steric repulsions between microspheres due to an adsorbed polymer," *Phys. Rev. E* **64**, 11401 (2001).
9. A. Ashkin, "Forces of a single-beam gradient trap on a dielectric sphere in the ray optics regime," *Biophys. J.* **61**, 569–582 (1992).
10. G. Roosen, "La levitation optique de spheres," *Can. J. Phys.* **57**, 1260–1279 (1979).
11. R. Gussgard, T. Lindmo, and I. Brevik, "Calculation of the trapping force in a strongly focused laser beam," *J. Opt. Soc. Am. B* **9**, 1922–1930 (1992).
12. J. P. Barton, D. R. Alexander, and S. A. Schaub, "Theoretical determination of net radiation force and torque for a spherical particle illuminated by a focused laser beam," *J. Appl. Phys.* **66**, 4594–4602 (1989).
13. A. Rohrbach and E. H. K. Stelzer, "Trapping forces, force constants, and potential depths for dielectric spheres in the presence of spherical aberrations," *Appl. Opt.* **41**, 2494–2507 (2002).
14. T. A. Nieminen, H. Rubinsztein-Dunlop, and N. R. Heckenberg, "Calculation and optical measurement of laser trapping forces on non-spherical particles," *J. Quant. Spectrosc. Radiat. Transfer* **70**, 627–637 (2001).
15. X. C. Yao, Z. L. Li, H. L. Guo, B. Y. Cheng, and D. Z. Zhang, "Effects of spherical aberration on optical trapping forces for Rayleigh particles," *Chin. Phys. Lett.* **18**, 432–434 (2001).
16. E. Fallman and O. Axner, "Influence of a glass–water interface on the on-axis trapping of micrometer-sized spherical objects by optical tweezers," *Appl. Opt.* **42**, 3915–3926 (2003).
17. V. Garces-Chavez, D. McGloin, H. Melville, W. Sibbett, and K. Dholakia, "Simultaneous micromanipulation in multiple planes using a self-reconstructing light beam," *Nature* **419**, 145–147 (2002).
18. D. G. Grier, "A revolution in optical manipulation," *Nature* **424**, 810–816 (2003).
19. Z. W. Sun, S. H. Xu, G. L. Dai, Y. M. Li, L. R. Lou, Q. S. Liu, and R. Z. Zhu, "A microscopic approach to studying colloidal stability," *J. Chem. Phys.* **119**, 2399–2405 (2003).